

## Composition of tetrahedrite-tennantite and 'schwazite' in the Schwaz silver mines, North Tyrol, Austria

T. ARLT\* AND L. W. DIAMOND

Mineralogisch-petrographisches Institut, Universität Bern, Baltzerstrasse 1, CH-3012 Bern, Switzerland

### ABSTRACT

The hydrothermal fahlore deposits of the Schwaz-Brixlegg district have been mined for silver and copper over many centuries and are famous as the type locality of the mercurian fahlore variety 'schwazite'. The ore is dominantly monomineralic fahlore and occurs as stratabound, discordant vein, and breccia bodies over a 20 km belt hosted mostly by the Devonian Schwaz Dolomite. The structural style of the mineralization is similar to that of Mississippi Valley type deposits.

This study presents the first electron microprobe analyses of the ores and reveals wide variations in fahlore compositions, from 35 to 100 wt.% tetrahedrite end-member in the solid solution series with tennantite. Sb and Zn contents vary between 12.1–28.0 wt.% and 0.1–7.6 wt.%, respectively. Silver contents average 0.5 wt.% and range up to 2.0 wt.%. In the breccia-hosted ores these variations clearly result from a temporal evolution in the ore-forming hydrothermal system: main-stage tetrahedrite is replaced by assemblages of Sb-, Fe-, and Ag-enriched tetrahedrite + enargite, with minor sphalerite  $\pm$  stibnite  $\pm$  cuprian pyrite ( $\leq$  25 wt.% Cu). These reactions are deduced to result from either increases in aqueous sulphur activity or falling temperature. Earlier workers recognized strong geographic zonation of fahlore compositions, but our microprobe analyses refute these contentions.

The 1167 new microprobe analyses of 51 fahlore samples collected underground or obtained from museum collections yield an average Hg content of 1.8 wt.%, and a maximum of 9.4 wt.%. According to modern nomenclature, not even the highest Hg value qualifies as 'schwazite'. Moreover, it appears that the original and only analysis of 'schwazite', reporting 15.6 wt.% Hg (Weidenbusch, 1849), was erroneously performed on a polyminerale aggregate, rather than on a monomineralic fahlore. We conclude that the Schwaz-Brixlegg fahlores are in fact not unusually rich in mercury, and that in all probability there is not, and never has been, any 'schwazite' at Schwaz.

**KEYWORDS:** Brixlegg, enargite, fahlore, mercury, Schwaz, schwazite, fukuchilite, silver, tetrahedrite-tennantite.

### Introduction

TETRAHEDRITE-TENNANTITE solid-solutions are the most common minerals of the fahlore group, they are the most widespread of all sulphosalts, and they are often important ores of silver (Charlat and Lévy, 1974; Johnson *et al.*, 1986; Sack, 1992). At Schwaz in Tyrol, large deposits of tetrahedrite-tennantite occur as stratabound, vein, and breccia bodies over a 20 km belt of the Devonian Schwaz Dolomite unit. The geometry and gangue mineralogy of the

deposits are reminiscent of Mississippi Valley-type base-metal deposits (Frimmel, 1991) but their genesis is disputed. Hypotheses range from syngenetic-sedimentary (Schulz, 1972; Gstrein, 1979; Schroll, 1979), through epigenetic-hydrothermal (Vohryzka, 1968; Tufar, 1979; Frimmel and Papesch, 1990; Frimmel, 1991), to karstification processes (Mostler, 1984). Although the average silver content of the fahlores is only 0.5 wt.%, the huge quantities of ore led the deposits to become the largest silver mines in Europe in the 15th and 16th centuries. Copper and silver mining ceased in the district in 1957 but baryte was extracted from the Kogel Mines until 1968. Very locally mercury was also exploited (Falkenstein Mine, Schwaz).

\* Present address: Bayerisches Geoinstitut, Universität Bayreuth, D-95440 Bayreuth, Germany

Now largely exhausted, the deposits are still of scientific interest because of the insight they may provide into mechanisms of ore genesis and hence to conceptual models for exploration.

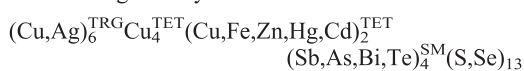
For example, Isser (1905; cited in Schmidegg, 1951) inferred the presence of a geographic trend in fahlore compositions in the Schwaz area, broadly analogous to the trends reported by Wu and Petersen (1977) in the regionally extensive vein deposits at Casapalca, Peru, and by Lynch (1989) in the Keno Hill District, Yukon. The trends at Casapalca have been postulated to reflect the flow paths of the ore-bearing solutions (Wu and Petersen, 1977; Hackbarth and Petersen, 1984). Documentation of the trends at Schwaz therefore offers the potential to map out flow paths which could serve as guides for further exploration.

The fahlore deposits at Schwaz are also of interest because they are the type-locality of the mercurian tetrahedrites termed 'schwazite'. While schwazite is widely known today, our literature survey revealed the peculiarity that, since the initial discovery of a tetrahedrite containing 15.6 wt.% mercury by Weidenbusch in 1849, no subsequent workers in the Schwaz deposits have been able to report an analysis of a fahlore with enough mercury to be classified as schwazite.

The purpose of the present mineralogical study is therefore threefold: (1) to establish the extent of chemical variation in fahlores of the Schwaz dolomite and to characterize their parageneses and reaction textures; (2) to verify the existence of the proposed compositional trend along the dolomite belt, and (3) to focus on the mercury contents of the fahlores in order to clarify the importance of schwazite at Schwaz.

### Chemistry and nomenclature of fahlores

The extent of compositional variation in fahlores has been investigated by Johnson *et al.* (1986) and Breskovska and Tarkian (1994). Their works compile the analyses of 1900 natural and synthetic samples, from which it appears that fahlore generally fits the formula:



Antimony and arsenic show complete mutual substitution on the semi-metal sites (SM) between the tetrahedrite ( $\text{Cu}_{12}\text{Sb}_4\text{S}_{13}$ ) and tennantite ( $\text{Cu}_{12}\text{As}_4\text{S}_{13}$ ) end-members. Other compositional end-members may be distinguished with respect to substitutions on the tetrahedral (TET) sites (e.g.

Seal *et al.*, 1990; Sack, 1992): ferroan tetrahedrite ( $\text{Cu}_{10}\text{Fe}_2\text{Sb}_4\text{S}_{13}$ ), zincian tetrahedrite ( $\text{Cu}_{10}\text{Zn}_2\text{Sb}_4\text{S}_{13}$ ) and mercurian tetrahedrite ( $\text{Cu}_{10}\text{Hg}_2\text{Sb}_4\text{S}_{13}$ ). The general formula above suggests that fahlore can accommodate a maximum of 6 Ag atoms per formula unit (p.f.u.) (e.g. freibergite,  $\text{Ag}_6\text{Cu}_4(\text{Cu,Fe,Zn,Hg})_2(\text{Sb,As})_4\text{S}_{13}$ ), all on the trigonal-planar (TRG) sites (Charnock *et al.*, 1989). This limit is largely borne out by the analyses of natural fahlores (Johnson *et al.*, 1986), although there are exceptions with nearly 10 Ag atoms p.f.u. (Charlat and Lévy, 1974; Patrick and Hall, 1983). The siting of the excess Ag in these cases is not yet clear.

Mercury-bearing fahlores are widely known as 'schwazite' (sometimes erroneously spelled 'schwartzite'), although this name is justifiably not recognized by the nomenclature commission of the International Mineralogical Association. The name 'schwazite' derived from the locality Schwaz in Tyrol, and was first introduced by Kenngott (1853), who reported a tetrahedrite analysis by Weidenbusch (1849) yielding the composition  $\text{Cu}_{9.9}\text{Hg}_{1.4}\text{Fe}_{0.7}\text{Zn}_{0.4}\text{Sb}_{3.2}\text{S}_{13}$  (15.57 wt.% Hg). The mercury content necessary to classify the fahlore as schwazite was not stipulated by Kenngott (1853), and so Schroll and Azer Ibrahim (1959) proposed that any fahlore with more than 10 wt.% Hg should be termed schwazite, whereas those with lower contents should be termed mercurian (or mercury-bearing) fahlore. Mozgova *et al.* (1980) later suggested applying a 50% rule for solid solutions on an atomic basis: thus the name schwazite should apply to any fahlore with one or more Hg atoms p.f.u., i.e.  $\text{Hg}_{1-2}\text{Cu}_{11-10}(\text{As,Sb})_4\text{S}_{13}$ . This scheme turns out to be very close to the older wt.% definition, because one atom p.f.u. corresponds to 10.33 wt.% Hg in tetrahedrite and 11.44 wt.% Hg in tennantite. According to either nomenclature, schwazite occurs in several localities: the Ord Mine, Arizona, USA (Faick, 1958); the Maskara deposit, Bosnia (Schroll and Azer Ibrahim, 1959); the Chaganuzun deposit, Gornyy Altai, Russian Federation (Vasil'yev and Lavrent'yev, 1973); the Chiproytsi deposit, NW Bulgaria (Atanasov, 1975), and the Gand and Leogang deposits in Austria (Götzinger *et al.*, 1985; Lengauer, 1988a). Other reports of schwazite consistent with the above definition are given by Kalbskopf (1971), Heidtke (1984) and Götzinger *et al.* (1997). Although most of the reported

TETRAHEDRITE-TENNANTITE COMPOSITIONS

schwazites are tetrahedrites, a tennantite has also been found at the Kul'pol'ney deposit, Chukotka, Russian Federation (Mozgova *et al.*, 1980).

The crystal structure of schwazite has been investigated by Kalbskopf (1971) and Kaplunnik *et al.* (1980). Hg was found to occupy the tetrahedral site while silver substitutes for Cu on the trigonal-planar site. Johnson *et al.* (1986) note that many natural fahlores contain traces of Hg, and these may be compositionally complex. However, samples rich in Hg tend to have a full complement of Cu, i.e.  $10 \pm 1$  atoms p.f.u., and hence they are usually poor in silver.

**Geological setting of the Schwaz fahlore deposits**

The Schwaz-Brixlegg mining district is located at the western margin of the East-Alpine Greywacke

Zone (Fig. 1). The Palaeozoic basement of the district is made up principally of the metagranitic Kellerjoch gneiss (also known as the Schwazer Augen-gneiss) and Upper Ordovician to Silurian clastic metasediments and alkalic volcanics. These are capped by the Schwaz Dolomite, a unit of Devonian platform carbonates up to 800 m thick (Pirkl, 1961). This Palaeozoic basement-cover complex was folded, faulted and metamorphosed at approximately 300°C and 2 kbar during the Hercynian orogeny (Lengauer, 1988b). The complex was subsequently covered by post-orogenic molasse and Permian clastic sediments (Buntsandstein), followed in the Triassic by deposition of shallow-water carbonates (labelled Northern Calcareous Alps in Fig. 1). During the mid-Tertiary Alpine orogeny both the Permo-Mesozoic sediments and the underlying Palaeozoic complex were weakly metamor-

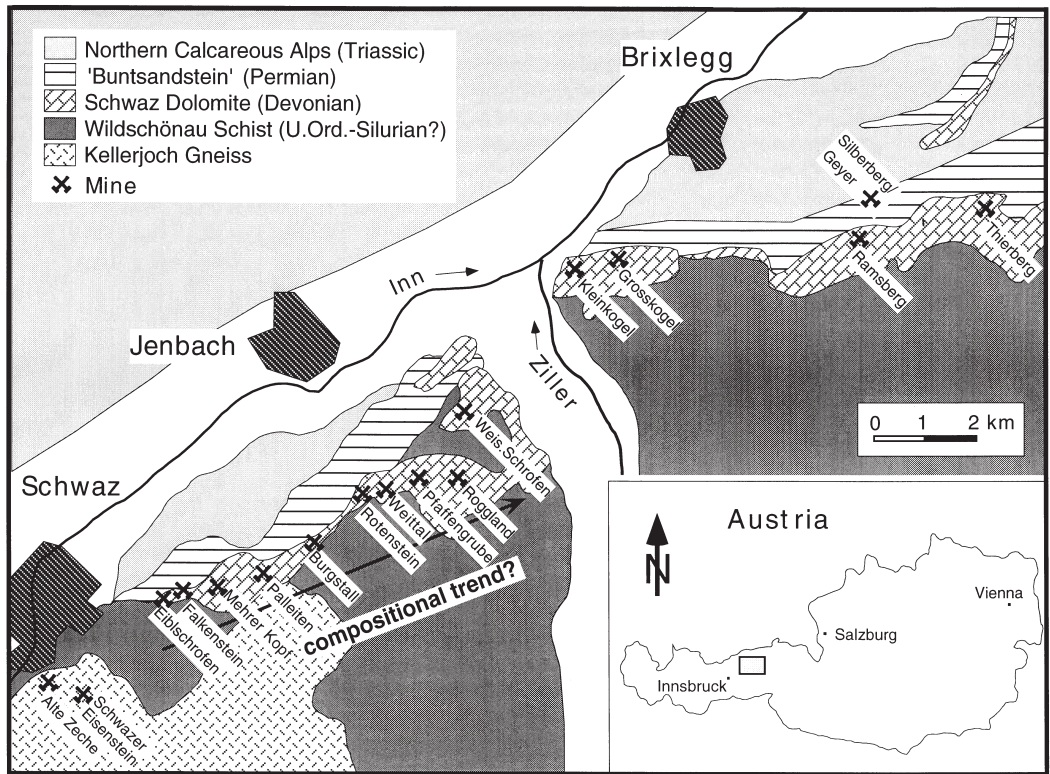


FIG. 1. Geology and location of silver mines in the Schwaz-Brixlegg district. The geographical trend in fahlore compositions (increasing Fe and Sb contents to the NE) proposed by Isser (1905) and Schmidegg (1951) is indicated by the arrow.

phosed, overturned and transported to their present location as part of the Upper Austroalpine nappes. Finally, the units were block-faulted during late Alpine uplift (the trace of the largest of these faults is marked by the Inn Valley, Fig. 1).

The most important argentiferous fahlore concentrations occur as stratabound, vein, and breccia bodies in the Schwaz Dolomite unit (Fig. 1). The deposits are distributed along a 20 km belt which runs north-east from Schwaz, roughly parallel to the Inn Valley Fault. The breccias in the Grosskogel mine are syn-depositional collapse structures which were originally filled with anhydrite. Sulphides and baryte appear to have replaced the anhydrite (Frimmel and Papesch, 1990). Other fahlore deposits are hosted by the Triassic sediments of Brixlegg, and tetrahedrite-bearing siderite veins have been mined in the Kellerjoch basement gneisses south-east of Schwaz.

The age of the deposits is disputed. Gstrein (1979) places the main ore-forming event in the mid-Devonian, in accord with his proposal that at least some of the ore bodies are of syngenetic origin, but Frimmel (1991), who investigated the baryte-bearing breccias in the Grosskogel Mine, favours epigenetic formation in the late Carboniferous. The minimum possible age of the main mineralization is well constrained by the occurrence of ore-bearing clasts of Schwaz dolomite in a breccia within the lowermost Triassic Reichenhaller Schists (Schober, 1984). All previous workers recognize very minor, localized remobilisation of the ores attributable to the effects of the Alpine orogeny (e.g. Schulz, 1979).

Although approximately 20 ore minerals have been described from the sulphide deposits in the Schwaz Dolomite (Grundmann and Martinek, 1994), most of them are volumetrically insignificant and are detectable only by microscopy. The main ore is essentially monomineralic fahlore in the area between Schwaz and the Ziller Valley (hereafter referred to as the Schwaz area), while between the Ziller Valley and Brixlegg (Fig. 1, referred to as the Brixlegg area) the fahlore is typically accompanied by minor enargite and/or luzonite (the high- and low-temperature polymorphs, respectively, of  $\text{Cu}_3(\text{As,Sb})\text{S}_4$ ; Haditsch and Mostler, 1969; Schober 1984; this study).

Little is known about the physicochemical processes and conditions of ore deposition in the Schwaz-Brixlegg district. Frimmel (1991) esti-

mated formation temperatures to lie between 70 and 130°C, based on Sr isotope analyses and calculated water:rock ratios, but our preliminary fluid inclusion analyses show that fahlore precipitated from a brine above 130°C and below 210°C (Arlt and Diamond, 1996).

#### Previous work on fahlores at Schwaz

Isser (1905) reported wet-chemical analyses of fahlores in the Schwaz Dolomite and inferred compositional trends along the mineralized belt (Fig. 2). The Sb content was reported to increase from south-west to north-east, while Zn and Hg contents decrease. Later workers (Schmidegg, 1951; Gstrein, 1978) cited these early data but also pointed out that fahlore compositions may vary locally, e.g. across individual fractures. Schroll and Azer Ibrahim (1959) also analysed fahlores from the Schwaz Dolomite by wet-chemical and spectroscopic methods, but their compositions show a large scatter which conflicts with the simple geographic trend reported by Isser (1905). Gstrein (1978) postulated variations in fahlore compositions on a centimetre scale, based on optical reflection measurements. Gstrein (1978) also noted that his XRF analyses yielded only weak variations in element contents, but he did not report any of the new data. Neuninger *et al.* (1960) presented several spectroscopic analyses of fahlores from Schwaz, but because their element ratios are clearly erroneous ( $\text{Ag} > \text{Sb}$ ), the data are not further discussed herein.

Fahlores from the Triassic sediments of the Brixlegg area (Fig. 1) have been investigated by Gstrein (1983) and Schober (1984). Gstrein (1983) inferred a compositional trend with stratigraphic level, based on semi-quantitative analyses, but the electron microprobe analyses of Schober (1984) show tennantites of rather constant composition. No data are available concerning the composition of fahlores in the siderite deposits of the Kellerjoch metagranitic gneisses.

Due to the citation of Kenngott (1853) in the early mineralogic encyclopediae (Zepharovich, 1859; Dana 1896), Schwaz is now famous as the type-locality of schwazite. However, Isser (1905, cited in Schmidegg, 1951) found a maximum Hg content of only 1.9 wt.% — well below the level that had hitherto been taken to qualify as schwazite. Similarly, Schroll and Azer Ibrahim (1959) found at most only 5.4 wt.% Hg in the 15 fahlores they analysed (average = 2 wt.% Hg). They conceded that their failure to find schwazite

TETRAHEDRITE-TENNANTITE COMPOSITIONS

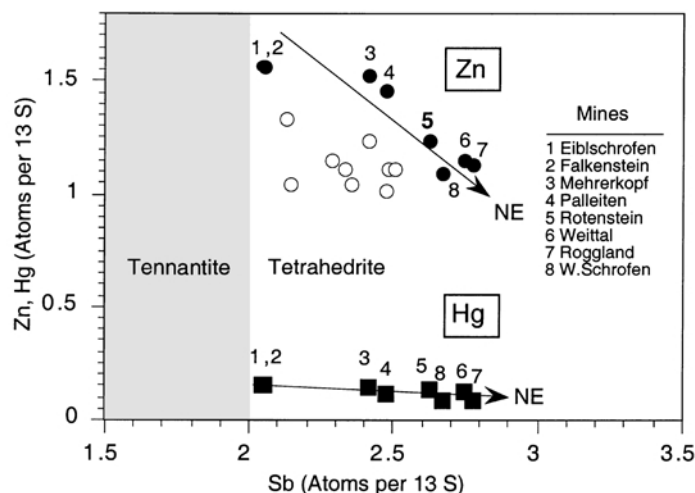


FIG. 2. Compositions of fahlore in the Schwaz Dolomite, taken from the literature. Open symbols, Brixlegg area (Schober, 1984); filled symbols, Schwaz area (Isser, 1905). Arrows indicate compositional trends from SW to NE according to Isser (1905). See Fig. 1 for locations of labelled mines.

may have been due to chance in sampling. Gstrein (1979, p. 188) reported that schwazite is the dominant ore in the Schwaz deposits, whereas tetrahedrite (*sic*) is rarer. This statement is remarkable, because Gstrein (1978, 1979) based his conclusion on the analyses of Isser (1905), which yielded only very minor Hg contents. Presumably Gstrein (1979) used the term 'schwazite' to signify fahlore with any detectable content of Hg. It thus appears that, despite considerable effort, none of the workers following Weidenbusch (1849) have been able to find a fahlore at Schwaz with more than 5.4 wt.% Hg.

#### Sampling and analytical procedure

The Grosskogel, Kleinkogel, and Rotenstein Mines in the Schwaz-Brixlegg area (Fig. 1) were chosen for detailed study because samples could be collected *in situ* underground and well documented. During sampling, careful attention was paid to differentiate the various ore geometries (e.g. stratabound, discordant, breccia). Two samples were also collected from veins in the Kellerjoch gneiss. In addition to our own samples, fahlores from historic collections were analysed, including material from the Joanneum Graz, the Natural History Museum of Vienna, the Natural History Museum of Bern, the Technical University of Munich, the Humboldt Collection in Potsdam and private

collections. The set was complemented by a sample from the Weisser-Schrofen Mine, Schwaz, which contains abundant secondary cinnabar and sample FaT24 from Krummörterrevier, the only locality where mercury was mined. A description of the investigated samples is given in Table 1.

Chemical compositions of the ores were determined with a CAMECA SX50 electron microprobe at the University of Bern. Natural tennantite, freibergite, arsenopyrite and cinnabar standards were used to calibrate quantitative analyses. The operating conditions were 15 kV accelerating potential, 20 nA beam current, and 25 sec X-ray peak acquisition times. Measurements were made with a tightly focussed beam on 10 to 50 spots per sample. Traverses were measured on two crystals of approximately 5 mm diameter from the Grosskogel mine. Short replicate analyses on the same spots showed that no diffusion of Ag occurred during the peak measurement time used for analysis (cf. Harris, 1990). The acquired X-ray intensities were corrected for atomic number, mass-absorption and secondary fluorescence effects using the CAMECA-PAP version of the Pouchou and Pichoir (1984) procedure.

The coexistence of enargite and luzonite in the Brixlegg samples was identified using a Philips PW 1800 X-ray diffractometer with Cu-K $\alpha$  radiation.

TABLE 1. Description of analysed fahlores from the Schwaz-Brixlegg mining district

Sample	Source	Locality	Description
Samples from Grosskogel and Kleinkogel Mines, Brixlegg area (Table 2)			
GKT1	New, AH	Kramst., Grosskogel	Freely grown crystal, with En/Luz, Cu-pyrite
GKT2	New	Kramst., Grosskogel	Idiomorphic crystal, with baryte, En/Luz
GKT12	New	Dilitzstollen, Grosskogel	Up to 30 vol% En/Luz
GKT14	New	Deepest point Bauernzeche; Grosskogel	Dolomite-breccie, with En/Luz
GK17	New, KPM	Kramst., Grosskogel	With chalcostibite, En/Luz
GKT19	New	Schwerspatzeche, Kramst., Grosskogel	
GKT20	New, RP	Kieszeche, Kramst., Grosskogel	Discordant, pyrite bearing vein
KKT3	New, RP	1. Sohle Kleinkogel-UB (Georgi-West)	With stibnite, Chalcostibnite, En/Luz
KKT6	New	Gabrielst., Kleinkogel	Idiomorphic crystals, with baryte
KKT15	New	2. Sohle Kleinkogel-UB; Auffahrt(-1)	With En/Luz and Cu-pyrite
HumF4	Berlin	Grosskogel, Brixlegg	Analyses provided by V. Lüders
Samples from Rotenstein Mine and others, Schwaz area (Table 3)			
RoT4	New	Sebastianst., 'Dreier' (StM 100)	Dolomite breccia
RoT5	New	Bartlmst., 'Dreier' (StM 250)	Recrystallised dolomite, qtz
RoT7	New	Grafenst., Grafengang	Small vein (2 cm wide),
RoT8	New, AH	Bartlmst., Grafengang	Discordant vein
RoT11	New	Mittlerer Grafenst.,	Stratabound horizon (Gstrein, 1979)
RoT22	New	Auffahrtst., 1st stope to Grundnerst.	Stratabound horizon (Gstrein, 1979)
WST21	New	Jakobst., Weiser Schrofen	Secondary cinnabar, qtz
FaT24	New	Nasse Zeche, Krummtrerr., Falkenstein	High lustre, Hg-exploration reported (Tab.4)
Museum samples labelled 'Schwaz' (and Brixlegg) (Table 4)			
1051	Graz	'Falkenstein, Schwaz'	Massive ore
1165	Graz	Falkenstein, Schwaz	Massive ore in dolomite
4013	Graz	Schwaz	Part of 3cm crystal on dolomite
7039	Graz	Schwaz	Part of 5cm crystal on dolomite
7268	Graz	Wilhelm-Erbst., Falkenstein	Crystal on dolomite, with chalcostibite
7317	Graz	Schwaz	Massive ore with qtz
7318	Graz	Schwaz	Massive ore in dolomite
7345	Graz	Schwaz	Massive ore in dolomite
7352	Graz	Falkenstein, Schwaz	Massive ore
7356	Graz	Schwaz	Crystal on dolomite
70761	Graz	Schwaz	Massive ore, high lustre, no dolomite
1167	Graz	'Falkenstein, Schwaz'	Massive ore in dolomite with baryte (Kogel?)
7351	Graz	'Falkenstein, Schwaz'	Massive ore in dolomite with baryte (Kogel?)
I3Bb1	Bern	Schwaz	With qtz, Tscharnier (1784) Collection
I3Bb2	Bern	Schwaz	In dolomite, Tscharnier (1784) Collection
I3Be1	Bern	Schwaz	In dolomite, Tscharnier (1784) Collection
BB33	KPM	Buchberg, prehist. settlement, Jenbach	Secondary cinnabar
SchT16	Freiberg	Schwaz	Massive ore
schTU1	Munich	Schwaz	Massive ore, Krantz ca. 1900
schTU2	Munich	Schwaz	Massive ore
schTU3	Munich	Schwaz	Massive ore
schTU4	Munich	Schwaz	Massive ore, AJ VIII 61, in dolomite
schTU5	Munich	Schwaz	Massive ore
W2683	Vienna	Wilhelm-Erbst., Falkenstein	Krummtergang
W140	Vienna	Schwaz	Massive ore
W320	Vienna	Schwaz	Massive ore
Wi 1	Vienna	Alter Bau, Falkenstein, Schwaz	Massive ore
HumF3	Berlin	Schwaz	Analyses provided by V. Lüders
Samples from siderite mines in Kellerjoch Gneiss (Table 5)			
AZ32	New, KPM	Reitlinger Erbs., Schwader Eisenstein	Siderite vein, with chalcopyrite, qtz
SET18	New	Johannist., Schwader Eisenstein	Siderite vein, with chalcopyrite, qtz

Abbreviations of sources: AH - A. Hanneberg; Berlin - Humbolt Collection; Bern - Natural History Museum of Bern; Freiberg - Staatl. Mineralienniederlage Freiberg; Graz - Joanneum Graz; KPM - K.-P. Martinek; Munich - Technical University of Munich; New - This study; RP - R. Pverlein; Vienna - Natural History Museum of Vienna.

## TETRAHEDRITE-TENNANTITE COMPOSITIONS

### Results

#### Ore parageneses

The following descriptions of the hydrothermal mineralogy are based on field observations and on petrographic examination of our own samples, plus information in the literature.

The mines in the Schwaz area (Fig. 1) consist of massive, essentially monomineralic fahlore, with rare stibnite ( $Sb_2S_3$ ), chalcocite ( $Cu_2S$ ), and ubiquitous pyrite in small quantities. The pyrite mostly exhibits a pentagono-dodecahedral habit; it is Cu-free and is clearly older than tetrahedrite. Identical pyrite of diagenetic origin is a common accessory in the immediately adjacent dolomite host rocks (Pirkl, 1961), and the pyrite in the ore bodies appears to be a simple relict of selective replacement of wall rock dolomite during the earliest stages of hydrothermal mineralization.

The mineralogy of the deposits in the Brixlegg area (Fig. 1) is more complicated, as exemplified by the assemblages in mineralized breccias in the Grosskogel Mine (Fig. 3). The earliest hydrothermal minerals are pyrite, derived from the wall rocks in the same manner as described above for the Schwaz deposits, plus recrystallized wall-rock dolomite. Small amounts of idiomorphic quartz overgrow the dolomite and pre-date the deposition of huge quantities of tetrahedrite (labelled 'I' in Fig. 3), plus minor quartz, dolomite and stibnite (occurring as inclusions in quartz). This main-stage paragenesis is followed by abundant baryte, or locally anhydrite (Frimmel, 1991).

A second generation of mineralisation may overgrow both baryte and tetrahedrite-I in the

Grosskogel breccias. It consists of quartz, present as idiomorphic crystals up to 2 mm diameter, dolomite, and intergrown tetrahedrite (labelled 'II' in Fig. 3), enargite/luzonite, stibnite, sphalerite and pyrite. The late pyrite, in contrast to the earlier generation, exhibits a light creamy tan colour in reflected light, it shows neither birefractance nor anisotropy, it is anhedral, and contains up to 25 mol.% Cu. The origin of this sulphide paragenesis is discussed in more detail below. In Fig. 3 we have assigned all these minerals to the pre-Triassic stage of mineralization, because the breccia clasts observed by Schober (1984) in the lowermost Triassic sediments contain enargite/luzonite in fractures within first-generation tetrahedrite.

Calcite and strontianite are obviously later than the paragenesis containing tetrahedrite-II, and Frimmel (1991) argued on Sr isotopic grounds that they precipitated during Alpine time. Krischker (1990) identified three types of baryte on the basis of their Sr contents, but we have not been able to assign these relative ages using petrographic criteria.

Secondary minerals are common in the studied mines but have been omitted from Fig. 3. Some of the sulphates occur as coatings on stope walls (e.g. langite, posnjacite, devilline and brochantite) and evidently these minerals have grown within the last 50 years.

#### Fahlore compositions

This study presents the first electron microprobe analyses of ores in the Schwaz area. The results of 1167 spot analyses on 51 samples are summarized

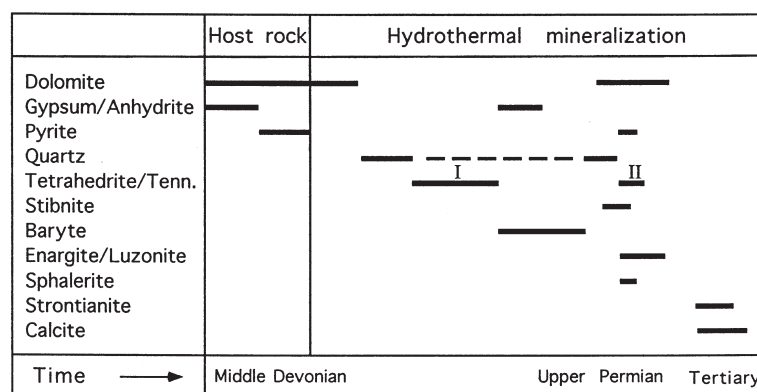


FIG. 3. Schematic paragenetic sequence in mineralized breccias of the Grosskogel Mine, Brixlegg area.

as averages and standard deviations in Tables 2–5, with all formulae calculated on the basis of 13 sulphur atoms. In addition to fahlores from the Schwaz Dolomite, Table 5 shows for comparison the analyses of two fahlore samples from the siderite veins in the Kellerjoch metagranites.

Most fahlores from the Schwaz-Brixlegg district are well described by the simplified formula  $(\text{Cu,Ag})_{10}(\text{Fe,Zn,Hg})_2(\text{Sb,As})_4\text{S}_{13}$ , in good agreement with the general stoichiometry of tetrahedrite-tennantite solid solution members deduced by Johnson *et al.* (1986). When normalized to 13 sulphur atoms, the total number of atoms in the analysed fahlores ranges between 28.7 and 30.2, a range which is commonly observed in fahlore deposits elsewhere. Figures 4–6 illustrate the compositional variations in terms of Ag, Zn, Hg and Sb contents.

The majority of the fahlores lie within the middle of the tetrahedrite-tennantite solid solution series (total range is 35–100 mol.% tetrahedrite end-member). Sb and As correlate negatively in the ranges 12.1–28.0 wt.% Sb (1.6–3.9 atoms p.f.u.) and 0.7–11.2 wt.% As (0.2–2.4 atoms p.f.u.). Thus true tennantites ( $\text{As} > \text{Sb}$ ) are found in both the Triassic sediments (Schober, 1984) and in the Schwaz dolomite deposits (this study).

Copper concentrations vary from 36.8 to 43.9 wt.% (9.8–11.1 atoms p.f.u.) and Ag ranges from 0.0–2.0 wt.% (0.00–0.32 atoms p.f.u.), with the average for main-stage tetrahedrite at approximately 0.5 wt.% (Fig. 4). In general, silver does not correlate with the Sb/As ratio, in contrast to other fahlore deposits (e.g. Miller and Craig, 1983; Ebel and Sack, 1991).

The concentrations of bivalent metals, Fe, Zn and Hg, are highly variable. Fe ranges over 0.0 to 5.7 wt.% (0.0–1.7 atoms p.f.u.) and correlates negatively with Zn, which spans almost the entire range possible for fahlores (0.1–7.6 wt.%, or 0.0–1.9 atoms p.f.u.). Hg varies from 0.0 to 9.4 wt.% (0.0–0.82 atoms p.f.u.). The Hg-richest samples (Wi1, 70761, TU4 and FaT24) do not show any correlation between Hg and Ag, Zn or Sb contents. Manganese concentrations are generally very low (0.0–0.7 wt.% or 0.0–0.2 atoms p.f.u.). We did not analyse for other trace components in our study, but the analyses of samples HumF3 and HumF4, provided by V. Lüders, list Co (0.1 wt.%), Ni (0.1 wt.%), Ga (0.01–0.02 wt.%), Pb (not detected), and Bi (0.10–0.19 wt.%).

The compositions of the fahlores show several trends with respect to locality and geometry of the

ore bodies, as described in the following paragraphs. The Hg content of the Grosskogel and Kleinkogel fahlores varies from zero up to 1.6 wt.% (GKT17-I; Table 2). The Hg content in the Rotenstein samples (Table 3) is at most 1.1 wt.% (RoT5), and sample WST21, which is thickly covered with secondary cinnabar, contains only 2.7 wt.% Hg. Sample FaT24 from the Nasse Zeche stope in the Falkenstein Mine, a locality with unusually Hg-rich fahlores according to Gstrein (pers. comm., 1996), contains 6.5 wt.% Hg.

In the Grosskogel and Kleinkogel Mines most of the samples were collected from the baryte-bearing breccias, which are described to be stratabound on a large scale (Krischker, 1990). In these breccias the main-stage fahlore has approximately equal concentrations of Sb and As. In contrast, the second-generation fahlore, which was identified by overgrowth textures, is markedly richer in Sb, Fe, and Ag (up to 1.8 wt.% Ag in sample GKT17-II; Figs. 4 and 6). Similarly Sb-enriched fahlores are found in a discordant vein in the Grosskogel Mine (sample GKT20, Kieszeche stope). The presence of the second generation of fahlore explains the bimodal nature of the compositional plots for samples GKT1, GKT17, KKT15 in Figs. 4 and 6.

Analogous variations in fahlore compositions are observed in the Rotenstein Mine (Fig. 5). Two samples of stratabound fahlore in a stratigraphically high horizon (samples RoT4, RoT5; 'Dreiervererzung', Gstrein, 1978), associated with coarse-grained, recrystallized dolomite (similar to Grosskogel), have compositions similar to the main-stage breccia ores of the Grosskogel Mine. By comparison, the fahlores in a discordant vein (Grafengang, samples RoT7, RoT8) are relatively enriched in Sb and Fe. A third compositional type of fahlore may be distinguished in the Rotenstein Mine according to its low Zn content ( $\text{Cu}_{10.2}\text{Ag}_{0.06}\text{Fe}_{1.2}\text{Zn}_{0.4}\text{Sb}_{2.6}\text{As}_{1.4}\text{S}_{13}$ ; samples RoT11, RoT22; Fig. 5). This ore fills narrow fractures in fine-grained, non-recrystallized dolomite, and is stratabound over several kilometres (Gstrein, 1979).

The fahlores from veins in the Kellerjoch metagranites showed, in sample SET18, a bimodal composition similar to the Grosskogel ores, and in sample AZ32, a composition close to pure tetrahedrite end-member. These fahlores thus have the highest Sb contents in the Schwaz-Brixlegg district (15.0–28.2 wt.%; As correlates negatively between 0.2 and 10.0 wt.%). Silver values (0.0 to 0.5 wt.%) are lower than the ores in

TABLE 2. Averaged electron microprobe analyses of fahlores from the Grosskugel and Kleinkugel Mines, Brixlegg area

Sample Spots	GKT1-I [52]	GKT1-II [22]	GKT2 [70]	GKT12 [19]	GKT14 [10]	GKT17-I [22]	GKT17-II [21]	GKT19 [23]	GKT20 [20]	KKT3 [48]	KKT6 [44]	KKT15-I [28]	KKT15-II [21]	HumF4* [40]
Cu (wt.%)	42.15(0.71)	40.38(1.88)	41.80(0.72)	41.08(0.61)	42.92(0.66)	39.79(0.52)	38.56(1.25)	40.75(0.94)	39.15(0.51)	41.70(0.60)	40.37(0.91)	40.62(0.77)	39.93(0.64)	41.38(0.33)
Ag	0.48(0.94)	0.78(0.23)	0.45(0.11)	0.27(0.14)	0.27(0.10)	0.58(0.10)	1.77(0.44)	0.42(0.07)	0.46(0.07)	0.65(0.09)	0.52(0.19)	0.44(0.17)	0.85(0.15)	0.37(0.06)
Fe	2.94(0.41)	5.17(2.22)	2.41(0.38)	2.17(0.28)	2.35(0.08)	0.43(0.40)	3.72(0.89)	1.65(0.27)	1.89(0.41)	1.74(0.21)	0.33(0.51)	1.38(0.62)	4.42(0.46)	2.23(0.13)
Zn	3.70(0.45)	1.76(1.62)	4.11(0.47)	4.77(0.36)	4.44(0.16)	6.76(0.50)	1.51(0.80)	4.88(0.15)	4.45(0.72)	5.01(0.29)	6.94(0.70)	5.67(0.69)	0.92(0.83)	4.66(0.14)
Hg	0.85(0.73)	0.45(0.77)	1.16(0.70)	0.73(0.58)	0.79(0.71)	1.61(0.71)	0.49(0.50)	1.13(0.57)	0.20(0.29)	0.78(0.65)	1.26(0.66)	0.69(0.60)	0.72(0.54)	0.67(0.15)
Mn	0.05(0.10)	0.05(0.10)	0.02(0.03)	0.02(0.03)	0.01(0.02)	0.03(0.04)	0.02(0.03)	0.01(0.02)	0.01(0.01)	0.01(0.02)	0.02(0.03)	0.04(0.03)	0.02(0.04)	0.00(0.01)
Sb	13.98(0.83)	19.98(3.03)	15.41(1.72)	14.82(0.56)	14.91(0.29)	17.00(1.38)	27.33(1.52)	14.78(0.97)	23.85(2.23)	15.57(0.75)	16.73(2.30)	14.52(2.83)	26.30(2.46)	15.15(0.58)
As	10.27(0.64)	5.78(1.76)	9.26(1.24)	9.61(0.62)	9.42(0.48)	8.29(1.01)	1.60(1.36)	10.17(0.72)	3.74(1.66)	9.24(0.65)	7.52(1.68)	10.86(2.38)	2.24(1.85)	10.24(0.45)
S	26.56(0.25)	25.50(0.59)	26.24(0.39)	26.39(0.18)	25.99(0.43)	25.69(0.43)	24.78(0.31)	26.47(0.21)	25.45(0.34)	26.04(0.30)	25.68(0.61)	26.35(0.50)	25.19(0.36)	26.02(0.18)
Total	100.98(0.96)	99.85(1.66)	100.86(0.89)	99.86(1.00)	101.10(1.02)	100.18(1.13)	99.80(0.91)	100.25(0.61)	99.21(0.55)	100.75(0.94)	99.37(1.24)	100.58(1.05)	100.57(0.97)	100.95
Cu	10.41(0.19)	10.39(0.45)	10.45(0.14)	10.21(0.13)	10.84(0.20)	10.16(0.20)	10.21(0.39)	10.10(0.23)	10.09(0.09)	10.50(0.17)	10.32(0.27)	10.11(0.18)	10.40(0.18)	10.43
Ag	0.07(0.39)	0.12(0.04)	0.07(0.02)	0.04(0.02)	0.04(0.02)	0.09(0.02)	0.28(0.02)	0.06(0.01)	0.07(0.01)	0.10(0.01)	0.08(0.03)	0.06(0.03)	0.13(0.02)	0.05
Fe	0.83(0.11)	1.52(0.66)	0.69(0.11)	0.61(0.08)	0.68(0.03)	0.12(0.11)	1.12(0.27)	0.46(0.07)	0.56(0.12)	0.50(0.06)	0.09(0.14)	0.39(0.18)	1.31(0.14)	0.64
Zn	0.89(0.11)	0.44(0.41)	1.00(0.11)	1.15(0.09)	1.09(0.02)	1.68(0.14)	0.39(0.20)	1.17(0.04)	1.12(0.17)	1.23(0.07)	1.72(0.18)	1.37(0.16)	0.23(0.21)	1.14
Hg	0.07(0.06)	0.04(0.06)	0.09(0.06)	0.06(0.05)	0.06(0.06)	0.13(0.06)	0.04(0.04)	0.09(0.04)	0.02(0.02)	0.06(0.05)	0.10(0.05)	0.05(0.05)	0.06(0.04)	0.05
Mn	0.01(0.03)	0.02(0.03)	0.01(0.01)	0.01(0.01)	0.00(0.01)	0.01(0.01)	0.01(0.01)	0.00(0.00)	0.00(0.00)	0.00(0.01)	0.01(0.01)	0.01(0.01)	0.01(0.01)	0
Sb	1.80(0.01)	2.69(0.42)	2.01(0.26)	1.92(0.08)	1.96(0.05)	2.27(0.20)	3.78(0.21)	1.91(0.14)	3.21(0.34)	2.05(0.10)	2.24(0.34)	1.89(0.40)	3.58(0.37)	1.99
As	2.15(0.14)	1.26(0.38)	1.96(0.25)	2.03(0.12)	2.02(0.11)	1.79(0.20)	0.36(0.30)	2.14(0.14)	0.81(0.35)	1.97(0.15)	1.63(0.35)	2.29(0.48)	0.49(0.40)	2.19
S	13.00	13.00	13.00	13.00	13.00	13.00	13.00	13.00	13.00	13.00	13.00	13.00	13.00	13.00
Total	29.23(0.23)	29.46(0.38)	29.27(0.20)	29.57(0.16)	29.69(0.25)	29.25(0.25)	29.18(0.30)	28.94(0.16)	28.88(0.14)	29.41(0.23)	29.18(0.29)	29.19(0.22)	29.21(0.21)	29.5

Numbers in square brackets are numbers of spot analyses per sample. Number in round brackets are standard deviations.

\* analyses provided by V. Lüders; Co = 0.01wt.%; Ni = 0.01wt.%; Ga = 0.02wt.%; Pb = 0.00wt.%; Bi = 0.19wt.%

TABLE 3. Averaged electron microprobe analyses of fahlores from the Rotenstein Mine and a Hg-rich locality at Weisser Schrofren Mine (WST21), Schwaz area

Sample Spots	RoT4 [56]	RoT5 [58]	RoT7 [51]	RoT8 [48]	RoT11 [17]	RoT22 [21]	WST21 [23]
Cu(wt.%)	41.13(0.56)	40.97(0.58)	40.34(0.68)	41.28(0.62)	41.25(0.58)	40.46(0.54)	39.11(0.74)
Ag	0.60(0.21)	0.47(0.09)	0.44(0.10)	0.28(0.06)	0.36(0.04)	0.53(0.18)	0.33(0.10)
Fe	1.22(0.10)	1.17(0.09)	2.72(0.40)	2.71(0.25)	4.09(0.21)	4.00(0.33)	0.56(0.13)
Zn	5.85(0.19)	5.92(0.13)	3.93(0.39)	4.14(0.16)	1.60(0.09)	1.47(0.08)	5.96(0.28)
Hg	1.03(0.74)	1.10(0.72)	0.83(0.70)	0.81(0.63)	0.68(0.72)	0.49(0.41)	2.70(0.60)
Mn	0.08(0.18)	0.07(0.13)	0.02(0.03)	0.01(0.02)	0.02(0.02)	0.01(0.01)	0.02(0.02)
Sb	14.76(0.65)	14.95(1.03)	21.13(2.13)	18.52(0.36)	19.74(0.46)	19.61(0.40)	16.28(1.68)
As	9.68(0.64)	9.50(0.79)	5.18(1.48)	7.22(0.40)	6.78(0.37)	6.89(0.46)	8.74(1.18)
S	26.10(0.37)	26.05(0.19)	25.35(0.42)	25.91(0.18)	26.33(0.19)	25.94(0.15)	25.74(0.28)
Total	100.47(1.05)	100.18(0.77)	99.93(1.16)	100.88(0.78)	100.85(0.83)	99.40(0.57)	99.44(0.84)
Cu	10.34(0.14)	10.32(0.14)	10.44(0.17)	10.45(0.13)	10.28(0.15)	10.23(0.13)	9.97(0.13)
Ag	0.09(0.03)	0.07(0.01)	0.07(0.02)	0.04(0.01)	0.05(0.01)	0.08(0.03)	0.05(0.01)
Fe	0.35(0.03)	0.33(0.03)	0.80(0.11)	0.78(0.07)	1.16(0.06)	1.15(0.10)	0.16(0.04)
Zn	1.43(0.04)	1.45(0.03)	0.99(0.10)	1.02(0.04)	0.39(0.02)	0.36(0.02)	1.48(0.06)
Hg	0.08(0.06)	0.09(0.06)	0.07(0.06)	0.06(0.05)	0.05(0.06)	0.04(0.03)	0.22(0.05)
Mn	0.02(0.05)	0.02(0.04)	0.00(0.01)	0.00(0.01)	0.01(0.01)	0.00(0.00)	0.00(0.01)
Sb	1.94(0.09)	1.97(0.14)	2.86(0.31)	2.45(0.05)	2.57(0.06)	2.59(0.05)	2.17(0.25)
As	2.06(0.14)	2.03(0.16)	1.13(0.31)	1.55(0.08)	1.43(0.08)	1.48(0.10)	1.89(0.24)
S	13.00	13.00	13.00	13.00	13.00	13.00	13.00
Total	29.32(0.26)	29.27(0.18)	29.36(0.21)	29.36(0.16)	28.94(0.14)	28.93(0.15)	28.94(0.17)

Numbers in square brackets are numbers of spot analyses per sample. Numbers in round brackets are standard deviations.

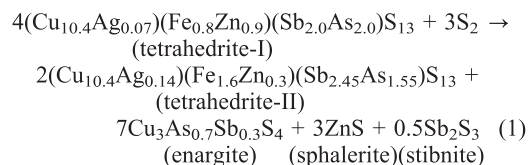
the Schwaz dolomite and are comparable to those in the Triassic metasediments (Fig. 4). Copper ranges from 36.6 to 39.8 wt.%, while the contents of bivalent metals are 1.9–3.8 wt.% Fe, 1.3–5.4 wt.% Zn, 0.0–6.3 wt.% Hg, and 0.0–0.1 wt.% Mn.

## Discussion

### Reactions involving tetrahedrite

The second-generation sulphide paragenesis in the Grosskogel breccias appears to be the product of a replacement reaction of the main-stage (first generation) tetrahedrite. The evidence for replacement is as follows. Tetrahedrite-II occurs intimately intergrown with small grains of enargite/luzonite, stibnite, sphalerite, and locally cuprian pyrite, in the rims of large first-generation tetrahedrite crystals (Fig. 7). The same assemblage is also found filling fractures within the first-generation tetrahedrite. In addition, second-generation tetrahedrite is occasionally present as monomineralic, idiomorphic overgrowths on segments of the polymineralic rims (Fig. 7), and

these overgrowths give the crystals a glossy lustre. In contrast, first generation tetrahedrite crystals without the monomineralic overgrowths or the rim sulphide paragenesis are distinctly matte. Finally, the tetrahedrite crystal zones hosting the late sulphide paragenesis are highly porous (Fig. 7). These features suggest that the first generation tetrahedrite dissolved along its rims and was locally replaced by the late sulphide assemblage, driving the fahlore solid-solution to Fe-, Sb-, and Ag-richer compositions. Electron microprobe measurements on enargite/luzonite yielded the averaged chemical formulae  $\text{Cu}_3\text{As}_{0.7}\text{Sb}_{0.3}\text{S}_4$ . Using selected mineral compositions, the continuous reaction can be written as follows:



TETRAHEDRITE-TENNANTITE COMPOSITIONS

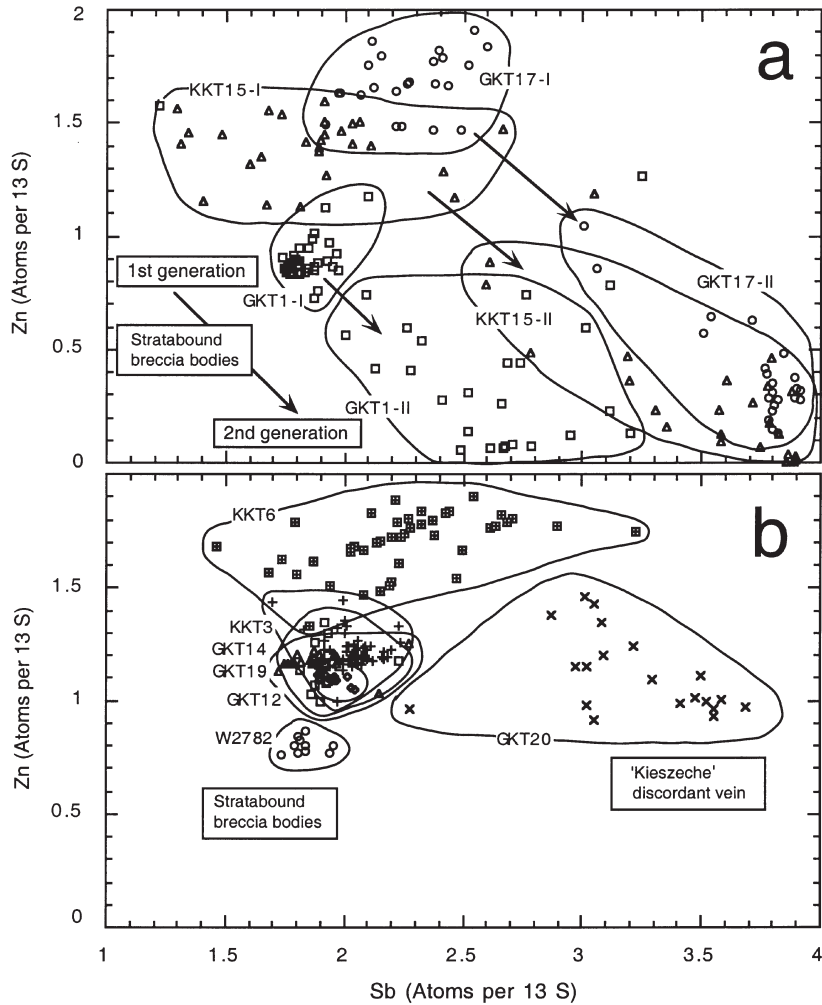


FIG. 4. Spot analyses of fahlores in the Grosskogel and Kleinkogel Mines, Brixlegg area (see Table 1 for sample descriptions). (a) Fahlores from stratabound fahlore-baryte-enargite breccias with bimodal compositions. Petrographic features show that this bimodality corresponds to two generations of fahlore growth (fields joined by arrows). (b) Fahlores from the same stratabound breccias as (a) showing no bimodality. Analyses from a discordant vein ('Kieszeche') are shown for comparison.

Thus the replacement of main-stage tetrahedrite could conceivably have occurred without additional net precipitation of metals from the hydrothermal fluid. The thermochemical data in Barton and Skinner (1979) and Seal *et al.* (1990) suggest that reaction 1 proceeds as written with increasing aqueous sulphur activity or decreasing temperature.

The stoichiometry of reaction 1 yields volumetric ratios of tetrahedrite-II/enargite/sphalerite/

stibnite of 17:13:2:1. These ratios compare approximately with optical estimates in some samples from the Grosskogel and Kleinkogel Mines, but certainly not in all. Most commonly, tetrahedrite-I is seen to give way to tetrahedrite-II + enargite, but additional solid phases necessary to balance the masses in the reaction are absent. In these samples it appears that the breakdown reaction was driven by a change in composition of the hydrothermal fluid, or by a significant

TABLE 4. Averaged electron microprobe analyses of Schwaz-Brixlegg fahlores in samples from museum collections

Sample	1051	1165	4013	7039	7268	7317	7318	7345	7352	7356	70761	1167	7351	FaT24
Spots	[9]	[12]	[11]	[12]	[14]	[14]	[10]	[12]	[17]	[12]	[18]	[11]	[12]	[25]
(wt.%)														
Cu	42.11(0.56)	40.10(0.69)	40.99(0.28)	41.84(0.40)	41.22(0.71)	41.49(0.49)	40.79(0.52)	41.79(0.56)	40.89(0.82)	40.52(0.52)	37.33(0.38)	41.94(0.37)	42.26(0.44)	38.44(0.62)
Ag	0.08(0.03)	0.66(0.30)	0.38(0.30)	0.39(0.05)	0.56(0.08)	0.55(0.09)	0.57(0.08)	0.49(0.11)	0.73(0.15)	0.72(0.23)	0.15(0.03)	0.81(0.44)	0.35(0.06)	0.76(0.46)
Fe	3.73(0.11)	0.99(0.21)	1.13(0.52)	2.47(0.52)	3.70(0.24)	2.88(0.15)	2.55(0.15)	3.09(0.13)	4.50(0.26)	3.12(0.17)	2.90(0.15)	2.60(0.19)	2.44(0.11)	1.34(0.12)
Zn	1.67(0.15)	6.12(0.15)	6.54(0.66)	4.47(0.14)	1.85(0.18)	3.00(0.09)	3.47(0.14)	2.99(0.12)	1.97(0.09)	2.45(0.11)	0.15(0.08)	4.28(0.29)	4.54(0.12)	3.34(0.20)
Hg	0.27(0.52)	1.49(0.76)	0.45(0.27)	1.05(0.52)	2.82(1.07)	1.06(0.56)	2.07(0.36)	0.95(0.51)	0.80(0.54)	2.95(0.54)	7.70(0.78)	0.39(0.33)	1.34(0.54)	6.47(0.90)
Mn	0.03(0.03)	0.02(0.02)	0.01(0.02)	0.01(0.02)	0.02(0.02)	0.02(0.03)	0.03(0.04)	0.02(0.03)	0.02(0.04)	0.01(0.03)	0.02(0.03)	0.03(0.03)	0.03(0.05)	0.01(0.02)
Sb	19.96(0.42)	17.48(1.09)	14.60(0.94)	14.65(0.32)	17.47(1.21)	18.77(0.58)	18.16(0.43)	18.60(0.52)	18.61(0.32)	12.78(1.07)	21.10(0.36)	14.02(0.65)	13.31(0.62)	17.29(0.84)
As	6.19(0.26)	7.67(1.01)	9.91(0.51)	10.09(0.43)	8.12(0.96)	6.99(0.42)	7.53(0.51)	7.21(0.52)	7.05(0.49)	10.45(1.01)	4.06(0.49)	10.37(0.35)	10.95(0.75)	7.75(0.72)
S	25.77(0.22)	25.43(0.18)	26.25(0.16)	26.32(0.14)	25.64(0.24)	25.76(0.17)	25.42(0.13)	25.70(0.16)	25.72(0.24)	26.01(0.25)	23.78(0.19)	26.34(0.13)	26.18(0.20)	24.93(0.22)
Total	99.82(0.82)	99.96(0.89)	100.27(1.11)	101.29(0.88)	101.38(1.05)	100.53(0.54)	100.59(0.72)	100.84(0.61)	100.29(0.87)	99.03(0.65)	97.19(0.58)	100.79(0.56)	101.40(0.70)	100.34(0.57)
Cu	10.72(0.15)	10.34(0.15)	10.25(0.07)	10.43(0.10)	10.55(0.17)	10.56(0.12)	10.53(0.13)	10.67(0.15)	10.43(0.19)	10.50(0.17)	10.30(0.12)	10.45(0.10)	10.59(0.11)	10.11(0.13)
Ag	0.01(0.01)	0.10(0.05)	0.06(0.02)	0.06(0.01)	0.08(0.01)	0.08(0.01)	0.09(0.01)	0.07(0.02)	0.11(0.02)	0.10(0.01)	0.02(0.01)	0.12(0.06)	0.05(0.01)	0.12(0.07)
Fe	1.08(0.04)	0.29(0.06)	0.32(0.15)	0.70(0.03)	1.08(0.06)	0.83(0.04)	0.75(0.04)	0.90(0.04)	1.31(0.07)	0.50(0.06)	0.91(0.04)	0.74(0.05)	0.70(0.03)	0.40(0.04)
Zn	0.41(0.04)	1.53(0.13)	1.59(0.16)	1.08(0.03)	0.46(0.05)	0.74(0.03)	0.87(0.04)	0.74(0.03)	0.49(0.02)	1.23(0.07)	0.04(0.02)	1.04(0.07)	1.11(0.03)	0.85(0.05)
Hg	0.02(0.04)	0.12(0.06)	0.04(0.02)	0.08(0.04)	0.23(0.09)	0.09(0.05)	0.17(0.03)	0.08(0.04)	0.07(0.04)	0.06(0.05)	0.67(0.07)	0.03(0.03)	0.11(0.04)	0.54(0.08)
Mn	0.01(0.01)	0.00(0.01)	0.00(0.01)	0.00(0.01)	0.00(0.01)	0.01(0.01)	0.01(0.01)	0.01(0.01)	0.01(0.01)	0.00(0.01)	0.01(0.01)	0.01(0.01)	0.01(0.01)	0.00(0.01)
Sb	2.65(0.07)	2.35(0.16)	1.90(0.11)	1.91(0.04)	2.33(0.18)	2.49(0.08)	2.45(0.07)	2.48(0.08)	2.48(0.05)	2.05(0.10)	3.04(0.07)	1.82(0.09)	1.74(0.09)	2.37(0.12)
As	1.34(0.05)	1.68(0.21)	2.10(0.11)	2.13(0.09)	1.76(0.20)	1.51(0.09)	1.65(0.11)	1.56(0.11)	1.52(0.10)	1.97(0.15)	0.95(0.11)	2.19(0.07)	2.33(0.15)	1.73(0.15)
S	13.00	13.00	13.00	13.00	13.00	13.00	13.00	13.00	13.00	13.00	13.00	13.00	13.00	13.00
Total	29.25(0.18)	29.43(0.18)	29.79(0.14)	29.95(0.19)	30.07(0.21)	29.89(0.15)	30.07(0.17)	30.08(0.15)	30.00(0.17)	29.41(0.23)	28.94(0.16)	29.95(0.09)	30.19(0.14)	29.14(0.14)

Numbers in square brackets are numbers of spot analyses per sample.

Numbers in round brackets are standard deviations

TABLE 4 *continued.* Averaged electron microprobe analyses of Schwaz-Brixlegg fahlores in samples from museum collections

	I3Bb1 [10]	I3Bb2 [12]	I3Be1 [12]	BB33 [19]	schT16 [14]	schTU1 [8]	schTU2 [8]	W320 [12]	schTU3 [11]	schTU5 [10]	schTU4a [15]	schTU4b [9]	W2683 [11]	Wil [13]	W140 [11]	HumF3* [40]
(wt.%)																
Cu	40.53(0.38)	40.67(0.44)	40.24(0.68)	40.21(0.77)	39.39(0.46)	40.38(0.73)	40.71(0.41)	40.58(0.49)	41.80(0.37)	41.19(0.51)	38.65(0.41)	41.12(0.39)	39.63(0.33)	37.63(0.37)	40.66(0.51)	41.52(0.74)
Ag	0.55(0.13)	0.38(0.07)	0.59(0.17)	0.36(0.16)	0.53(0.07)	0.32(0.07)	0.32(0.15)	0.80(0.17)	0.51(0.05)	0.38(0.05)	0.65(0.09)	0.36(0.05)	0.61(0.04)	0.86(0.17)	0.26(0.08)	0.54(0.05)
Fe	2.60(0.29)	1.62(0.07)	1.61(0.27)	1.26(0.24)	2.30(0.11)	1.83(0.08)	3.59(0.17)	3.28(0.10)	3.41(0.17)	2.00(0.11)	1.70(0.13)	1.92(0.13)	2.46(0.11)	0.41(0.09)	2.79(0.15)	2.94(0.25)
Zn	4.10(0.28)	5.28(0.13)	5.33(0.25)	5.68(0.24)	4.10(0.14)	5.11(0.18)	3.91(0.10)	1.74(0.07)	2.33(0.28)	4.57(0.12)	3.31(0.10)	4.69(0.13)	2.62(0.10)	4.30(0.09)	2.57(0.12)	3.74(0.42)
Hg	2.31(0.65)	2.18(0.47)	2.27(0.67)	2.17(0.72)	2.28(0.54)	0.43(0.61)	0.76(0.63)	2.51(0.67)	0.99(0.61)	0.89(0.37)	6.67(0.72)	1.54(0.58)	4.80(0.57)	8.46(0.80)	3.69(0.59)	0.68(0.20)
Mn	0.01(0.02)	0.02(0.02)	0.02(0.02)	0.01(0.03)	0.01(0.01)	0.02(0.02)	0.01(0.02)	0.01(0.02)	0.01(0.01)	0.03(0.04)	0.02(0.02)	0.02(0.02)	0.01(0.03)	0.04(0.04)	0.02(0.03)	0.00(0.00)
Sb	15.32(1.12)	13.96(0.25)	15.32(1.64)	15.60(1.66)	16.78(0.66)	18.04(0.90)	15.24(1.06)	18.80(0.34)	18.68(0.16)	17.13(0.51)	17.77(0.64)	18.24(1.34)	17.31(0.43)	18.53(0.17)	18.44(0.34)	14.97(1.07)
As	9.90(0.82)	10.58(0.46)	9.57(1.24)	9.63(1.31)	8.03(0.67)	8.00(0.62)	9.99(0.78)	7.08(0.39)	7.53(0.42)	8.59(0.50)	7.54(0.57)	7.89(0.92)	8.00(0.59)	6.49(0.30)	7.17(0.50)	10.45(0.77)
S	26.08(0.23)	26.18(0.16)	25.98(0.30)	25.82(0.38)	25.69(0.21)	26.28(0.30)	26.72(0.25)	25.49(0.12)	25.70(0.17)	26.20(0.16)	24.79(0.16)	25.85(0.25)	25.38(0.24)	24.10(0.17)	25.59(0.20)	26.24(0.52)
Total	101.40(0.63)	100.89(0.81)	100.90(0.85)	100.75(0.94)	99.12(0.66)	100.40(0.97)	101.23(0.67)	100.29(0.92)	100.97(0.75)	100.97(0.54)	101.08(0.73)	101.62(0.56)	100.83(0.59)	100.81(0.85)	101.18(0.72)	101.21
Cu	10.19(0.07)	10.19(0.14)	10.16(0.15)	10.22(0.13)	10.06(0.13)	10.08(0.18)	10.00(0.12)	10.45(0.14)	10.67(0.12)	10.31(0.11)	10.23(0.11)	10.44(0.13)	10.25(0.10)	10.24(0.09)	10.42(0.19)	10.38
Ag	0.08(0.02)	0.06(0.01)	0.09(0.03)	0.05(0.03)	0.08(0.01)	0.05(0.01)	0.05(0.02)	0.12(0.03)	0.08(0.01)	0.06(0.01)	0.10(0.01)	0.05(0.01)	0.09(0.01)	0.14(0.03)	0.04(0.01)	0.08
Fe	0.74(0.08)	0.46(0.02)	0.46(0.07)	0.36(0.07)	0.67(0.03)	0.52(0.02)	1.00(0.05)	0.96(0.03)	0.99(0.05)	0.57(0.03)	0.51(0.04)	0.55(0.03)	0.72(0.03)	0.13(0.03)	0.81(0.04)	0.84
Zn	1.00(0.07)	1.29(0.03)	1.31(0.07)	1.40(0.06)	1.02(0.04)	1.24(0.05)	0.93(0.03)	0.43(0.02)	0.58(0.07)	1.11(0.03)	0.85(0.02)	1.16(0.04)	0.66(0.02)	1.14(0.02)	0.64(0.03)	0.91
Hg	0.18(0.05)	0.17(0.04)	0.18(0.05)	0.17(0.06)	0.18(0.04)	0.03(0.05)	0.06(0.05)	0.21(0.05)	0.08(0.05)	0.07(0.03)	0.56(0.06)	0.12(0.05)	0.39(0.05)	0.73(0.07)	0.30(0.05)	0.05
Mn	0.00(0.00)	0.01(0.01)	0.00(0.01)	0.00(0.01)	0.00(0.00)	0.01(0.01)	0.00(0.00)	0.00(0.00)	0.00(0.00)	0.01(0.01)	0.01(0.01)	0.00(0.01)	0.00(0.01)	0.01(0.01)	0.01(0.01)	0
Sb	2.01(0.16)	1.83(0.03)	2.02(0.24)	2.07(0.24)	2.24(0.10)	2.35(0.13)	1.95(0.15)	2.53(0.05)	2.49(0.03)	2.24(0.07)	2.45(0.10)	2.42(0.20)	2.34(0.07)	2.63(0.03)	2.47(0.05)	1.96
As	2.11(0.16)	2.25(0.10)	2.05(0.24)	2.08(0.28)	1.74(0.14)	1.69(0.12)	2.08(0.15)	1.55(0.09)	1.63(0.09)	1.82(0.10)	1.69(0.12)	1.70(0.18)	1.75(0.12)	1.50(0.07)	1.56(0.10)	2.22
S	13.00	13.00	13.00	13.00	13.00	13.00	13.00	13.00	13.00	13.00	13.00	13.00	31.00	13.00	13.00	13.00
Total	29.33(0.14)	29.25(0.19)	29.27(0.18)	29.36(0.24)	28.99(0.16)	28.97(0.23)	29.07(0.19)	29.24(0.22)	29.52(0.15)	29.19(0.11)	29.40(0.12)	29.44(0.16)	29.21(0.15)	29.52(0.11)	29.25(0.18)	29.45

Numbers in square brackets are numbers of spot analyses per sample. Numbers in round brackets are standard deviations.  
\* analyses provided by V. Luiders; Co = 0.01 wt.%; Ni = 0.01 wt.%; Ga = 0.01 wt.%; Pb = 0.00 wt.%; Bi = 0.10 wt.%

TABLE 5. Averaged electron microprobe analyses of fahlores in two samples from Kellerjoch Gneiss SE of Schwaz

Sample Spots	AZ32 [17]	SET18-I [9]	SET18-II [13]
Cu(wt.%)	38.10(0.66)	39.50(0.78)	37.55(0.84)
Ag	0.04(0.04)	0.24(0.09)	0.33(0.09)
Fe	2.52(0.94)	3.49(0.22)	2.87(0.43)
Zn	4.48(1.30)	3.43(0.17)	3.54(1.08)
Hg	1.58(1.43)	1.04(0.61)	2.41(1.92)
Mn	0.02(0.02)	0.02(0.01)	0.02(0.02)
Sb	26.62(1.05)	16.57(0.95)	23.63(0.91)
As	1.46(0.74)	9.10(0.89)	3.64(0.94)
S	24.71(0.27)	26.25(0.26)	24.93(0.59)
Total	99.53(1.06)	99.65(0.66)	98.91(0.77)
Cu	10.12(0.14)	9.87(0.14)	9.88(0.15)
Ag	0.01(0.01)	0.04(0.01)	0.05(0.02)
Fe	0.76(0.29)	0.99(0.07)	0.86(0.15)
Zn	1.16(0.33)	0.83(0.04)	0.90(0.27)
Hg	0.13(0.12)	0.08(0.05)	0.20(0.17)
Mn	0.01(0.01)	0.00(0.00)	0.00(0.00)
Sb	3.69(0.17)	2.16(0.14)	3.25(0.20)
As	0.33(0.17)	1.93(0.18)	0.81(0.20)
S	13.00	13.00	13.00
Total	29.20(0.23)	28.91(0.14)	28.96(0.29)

Numbers in square brackets are numbers of spot analyses per sample. Numbers in round brackets are standard deviations

change in temperature (enough to alter relative solubilities of the component metals). Evidence to distinguish these possibilities is not available at present.

The presence of cuprian pyrite in this assemblage confirms the fluid inclusion evidence (Arlt and Diamond, 1996) for relatively low formation temperatures. Although pure  $\text{CuS}_2$  with pyrite structure is stable only under very high pressures (Schmid-Beurmann and Bente, 1995), metastable  $\text{FeS}_2\text{-CuS}_2$  solid-solutions (*in lieu* of stable  $\text{FeS}_2$  + covellite) have been observed to form in both nature and experiment at temperatures below  $275^\circ\text{C}$  (e.g. fukuchilite,  $\text{Cu}_3\text{FeS}_8$ , Kajiwar, 1969; Moh *et al.*, 1989; Oudin *et al.*, 1990; Shimazaki and Clark, 1970).

#### Temporal trends in fahlore compositions?

The bimodal fahlore compositions in breccias from the Grosskogel and Kleinkogel mines

clearly represent a temporal succession, as implied by reaction 1 above. Comparably bimodal compositions are found in the Rotenstein mine, but there the bimodality arises from comparing samples from different geometric types of ore — stratabound on the one hand, and discordant vein on the other. There is no field evidence for the relative ages of the two ore types, and since individual samples are not bimodal, there is no petrographic evidence either. By analogy with the temporal succession in the Grosskogel breccias, the discordant veins at Rotenstein could be inferred to be younger. However, the sulphides accompanying tetrahedrite-II in the product assemblage of reaction 1 are lacking from the discordant veins at Rotenstein. Indeed, one of the salient features of the mineralized district is the abundance of enargite in the Brixlegg area, and its absence from the Schwaz area. Thus regardless of the relative timing of the ore types, changes in bulk chemistry of the hydrothermal fluid must be invoked at Rotenstein to account for the compositional variations of the fahlores. The same conclusion applies to the discordant veins in the Grosskogel mine and in the Kellerjoch gneiss, where the fahlores have compositions similar to tetrahedrite-II in the Grosskogel breccias, but where enargite and other second-generation sulphides are likewise absent.

#### Geographical trends in fahlore compositions?

Based on bulk analyses, Isser (1905) and Schmidegg (1951) contended that the fahlores show a compositional trend with geographic location along the mineralized belt between Schwaz and the Ziller Valley (Fig. 2). However, our spot analyses of fahlores from the Rotenstein mine display the same range in composition as that seen through the entire ore district (Fig. 5, compare with Fig. 2 at the same scale). The wide spread in compositions at the same locality is still apparent even when the spot analyses are averaged to simulate bulk analyses. This result clearly refutes the existence of the geographical zonation in fahlore compositions proposed by Isser (1905). We conclude that Isser's (1905) inference of a compositional trend must have been based on fortuitous sampling.

Wu and Petersen (1977) discovered clear geographical trends in fahlore compositions at Casapalca, Peru, by comparing individual crystal growth zones at various localities in the same

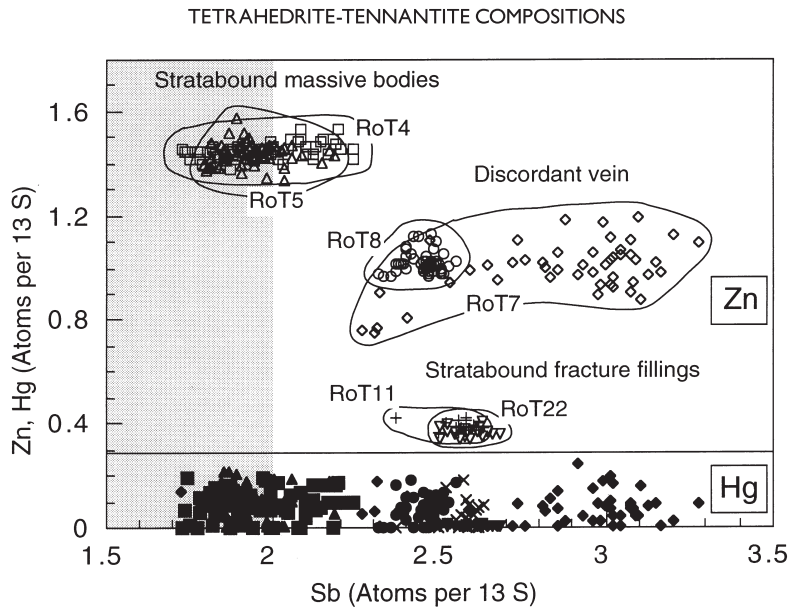


FIG. 5. Spot analyses of fahlores from the Rotenstein Mine, Schwaz area. Samples show different compositions according to ore geometry. The range in compositions in this mine is comparable to that of the entire ore district (compare with Fig. 2 at the same scale).

hydrothermal system. Such geographical zonation could indeed exist in the Schwaz-Brixlegg district, but the fahlore textures do not permit the necessarily detailed petrographic correlations to be performed.

*'Schwazite' at Schwaz?*

Neither we nor previous workers have been able to find significant amounts of mercury in samples from the Schwaz and Brixlegg areas. Therefore, 30 samples from historical collections were

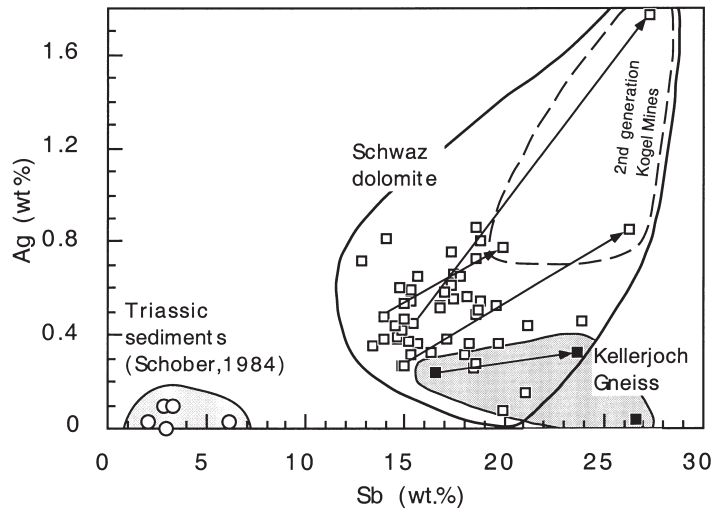
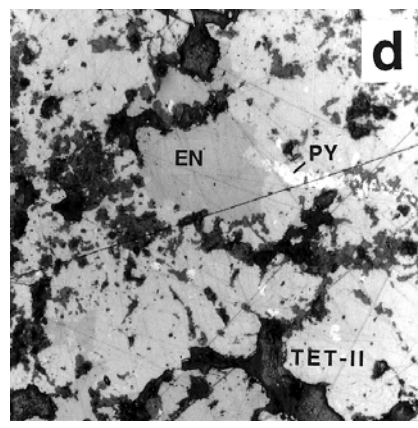
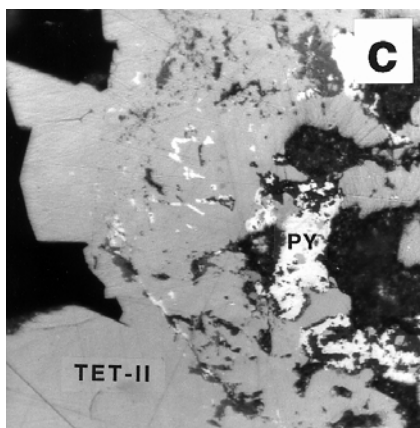
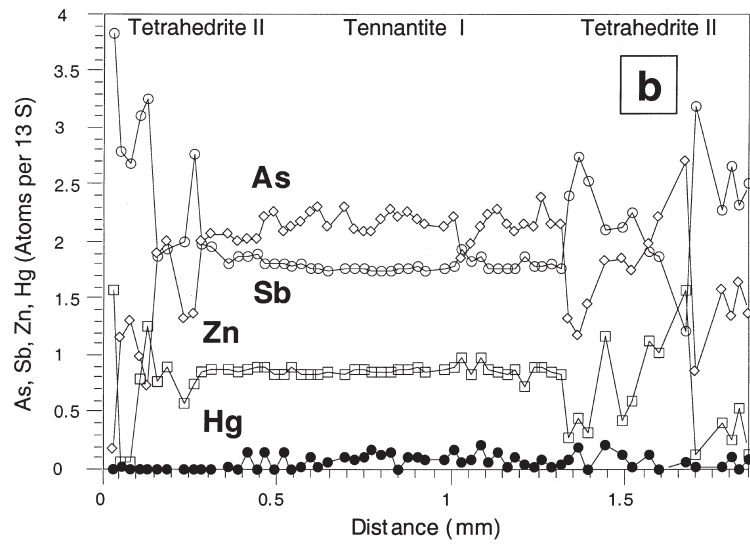
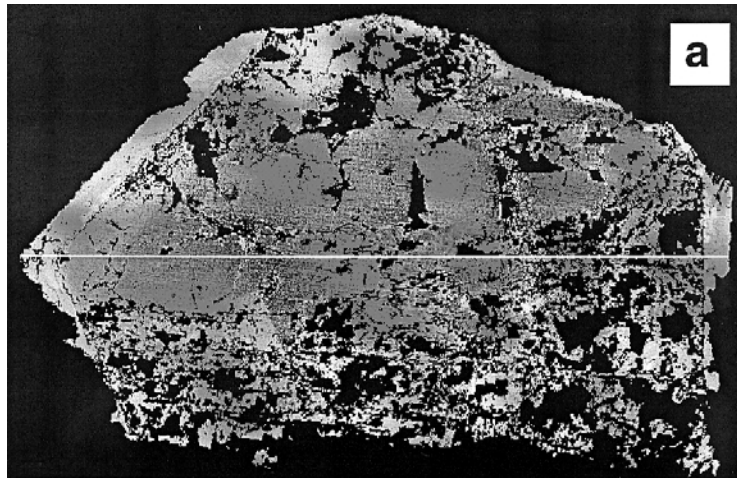


FIG. 6. Compilation of average compositions of fahlores from the Schwaz-Brixlegg district. Circles, Schober (1984); squares, this study (51 samples). Arrows join first and second generations of crystal growth in samples from the Grosskogel Mine (cf. Fig. 4a).



## TETRAHEDRITE-TENNANTITE COMPOSITIONS

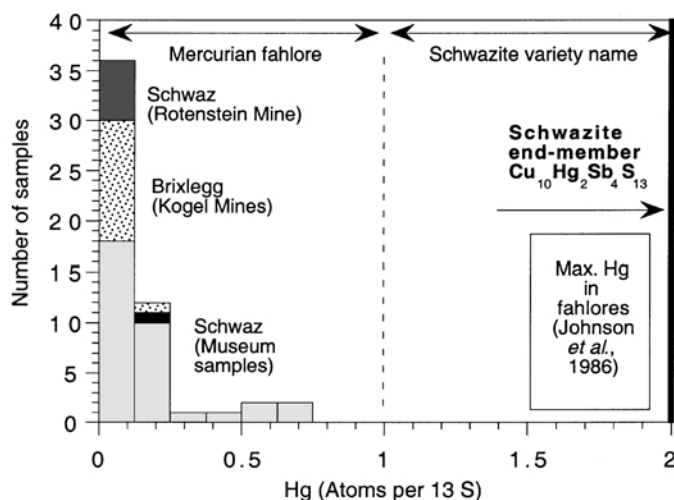


FIG. 8. Mercury contents of fahlores from the Schwaz-Brixlegg district. Light grey fields represent the museum samples presented in Table 4 (Schwaz), dark grey fields represent data from Rotenstein Mine, Schwaz area (Table 3) and points represent the samples of the Kogel Mines, Brixlegg area. None of the samples qualify as 'Schwazite'.

analysed to see if they have higher Hg concentrations. Most of the samples we obtained were originally labelled as 'schwazite' or 'mercurian fahlore' from 'Schwaz' or from 'Falkenstein' (the most productive mine in the Schwaz area and the only one from which mercury was exploited, according to the historical literature). Our microprobe analyses of these samples are somewhat surprising. Just as in our own samples collected *in situ*, most of the museum samples showed mercury contents between 0.3 and 3 wt.% (Table 4 and Fig. 8). This is approximately a tenth of the maximum possible Hg content in fahlores according to Johnson *et al.* (1986). Only three of the museum samples showed clearly higher values. The historical samples that are richest in Hg exhibit high lustre and conchoidal fracture, whereas the Hg-poorer samples have poor lustre and grainy fracture. We believe that some of the museum

samples labelled with the locality 'Schwaz' (samples 1167 and 7351) in fact derive from the Brixlegg area (e.g. Grosskogel Mine) because they contain the typical association of baryte + enargite.

Our compilation of all known analyses of the Schwaz-Brixlegg fahlores in Fig. 8 shows that the maximum average Hg content is 8.5 wt.%, and that the highest spot analysis is 9.4 wt.% (sample W11). Thus, using the definition of Mozgova *et al.* (1980), the Schwaz fahlores contain at most 40 mol.% schwazite end-member, and hence none of them qualify as 'schwazite'. The Hg content of the vast majority of the Schwaz fahlores is on the order of 2 wt.% and does not justify any special variety name.

These results led us to ponder the significance of the original analysis of schwazite by Weidenbusch (1849), which yielded 15.57 wt.% Hg. Two clues allow us to speculate on where the

FIG. 7. Fahlore crystal from a breccia in the Grosskogel Mine, Brixlegg area (sample GKT1). (a) Backscattered-electron image showing dark Sb- and Fe-poor core (TET-I) and light Sb- and Fe-rich rim (TET-II). Inner zone of rim contains numerous pores (black) and sulphide inclusions (see c). Outermost zone of rim is free of pores. These textures and mineral assemblages are interpreted to reflect replacement of the core tetrahedrite, as discussed in the text. (b) Quantitative electron microprobe analyses along the traverse indicated in (a). Spots which do not correspond to fahlore compositions (e.g. pores or other sulphides) have been omitted. (c) Detail of rim in (a): TET-II, second-generation tetrahedrite; PY, cuprian pyrite. Pores and crystal edge (dark areas) are outlined by idiomorphic tetrahedrite. (d) Detail of porous rim zone in a fahlore from the Kleinkogel Mine (sample KKT15). TET-II, second-generation tetrahedrite; PY, cuprian pyrite; EN, enargite. Lengths of pictures (c) and (d) correspond to 0.2 mm.

famous sample was collected: (1) Weidenbusch mentioned that his fahlore was associated with quartz and chalcopyrite. These are common phases in the siderite deposits in the Kellerjoch metagranites south of Schwaz city, whereas chalcopyrite is rarely found in the main mines hosted by dolomite; (2) The As content in Weidenbusch's analysis is almost negligible, whereas all other studies have shown that this is never the case for fahlores in the Schwaz Dolomite. As far as we are aware, only fahlore from Schwader Eisenstein, a siderite deposit in the Kellerjoch metagranites (sample AZ32, Table 1) is comparably poor in As. It therefore seems most likely that Weidenbusch's sample came from one of the deposits in the metagranites and not from the main carbonate-hosted fahlore deposits, as was assumed by Schmidegg (1951) and Gstrein (1983).

Weidenbusch (1849) reported that he was unable to extract all of the mercury simply by heating, and reaction with soda was necessary to separate the remainder. Both Weidenbusch (1849) and Rammelsberg (1849) discussed whether this might be due to the presence of a second Hg-bearing phase in the sample. By normalising the analysis of Weidenbusch (1849) to 13 sulphur atoms, we find that the sum of Hg + Fe + Zn is 2.5 atoms p.f.u. and the concentration of Sb is 3.2 atoms. The resulting ratio, 2:2.6, contrasts with the normal ratio in fahlores of 2:4 atoms. It therefore appears probable that the analysed sample indeed consisted of two different phases, rather than of one Hg-rich tetrahedrite.

We conclude that not even Weidenbusch (1849) discovered 'schwazite', according to the definition it was later given. Nevertheless, the discovery of a schwazite that fits the modern definition in the Leogang mining district (Lengauer, 1988a), approximately 80 km north-east of Schwaz, demonstrates that schwazite is actually present in the East-Alpine Greywacke zone.

## Conclusions

Electron microprobe analyses of a large number of samples have revealed wide variations in fahlore compositions in the Schwaz-Brixlegg district. In the breccias in the Grosskogel and Kleinkogel mines these variations clearly represent a temporal evolution in the hydrothermal system responsible for ore formation: main-stage tetrahedrite is replaced *in situ* by an assemblage

consisting of Sb-, Fe-, and Ag-enriched tetrahedrite + enargite  $\pm$  sphalerite  $\pm$  stibnite  $\pm$  cuprian-pyrite. In some samples the reaction can be balanced by the solid phases, but in others a change in fluid composition and/or temperature must be invoked to explain the second-generation tetrahedrite compositions. Similar differences in fahlore compositions have been found between the various types of ore bodies (stratabound, breccia and discordant vein) at given localities. These variations may also represent a temporal evolution in fluid properties, but evidence for the relative timing of the ore bodies is so far lacking.

A geographic trend in fahlore compositions in the Schwaz area was proposed by early workers, and the potential consequences of this for understanding the genesis of the ores was one of the main motivations behind the present study. However, our analyses demonstrate that there is in fact no geographical trend in fahlore compositions, at least as it was originally proposed. In principle, a subtle chemical zonation across the district may be indeed present, but the lack of ubiquitous, well-crystallized fahlore precludes the necessary petrographic correlations for its proof.

Schwaz is widely known as the type locality of the mercurian-fahlore variety 'schwazite'. However, we conclude that, according to modern nomenclature, there is not, and most probably never has been, any schwazite at Schwaz. It is debatable whether the *absence* of a mineral can ever be positively demonstrated, but we base our conclusion on a considerable number of analyses of both modern samples collected underground and of historical samples in museum collections. Moreover, we have been able to show that the original wet-chemical analysis of Weidenbusch (1849), which first reported a high mercury content in a fahlore from Schwaz, was in all probability performed on a polymineralic aggregate, rather than on a monomineralic fahlore. The case of 'schwazite from Schwaz' is thus one of several in the literature in which the initial find of a mineral later proved to be erroneous, but its report nevertheless stimulated the search and discovery of the mineral at other localities.

## Acknowledgements

We are grateful to the following persons and institutions for providing us with samples: H.-P. Bojar (Joanneum Graz), G. Grundmann (Technical University of Munich.), B.A.

TETRAHEDRITE-TENNANTITE COMPOSITIONS

- Hofmann (Natural History Museum of Bern), V. Lüdgers (Geoforschungszentrum Potsdam), G. Niedermayr (Natural History Museum of Vienna), P. Leblhuber and W. H. Paar (Salzburg University), A. Hanneberg, K.-P. Martinek and R. Pöverlein. The comments of B. Hofmann and F. Melcher, and reviews by J.F.W. Bowles and an anonymous referee, helped improve the manuscript. Support from the Swiss Science Foundation (Credit 21-26579.89 to M. Engi) is acknowledged for the electron microprobe laboratory at the University of Bern. T. Arlt is indebted to the Schweizerischer Nationalfonds for financial support (Credit 20-33562.92 to T. Peters).
- References**
- Arlt, T. and Diamond, L.W. (1996) Composition and formation conditions of tetrahedrite-tennantite in the Devonian Schwaz Dolomite, N-Tyrol, Austria. *Mitt. Österr. Mineral. Ges.*, **141**, 58–9.
- Atanasov, V.A. (1975) Argentinian mercurian tetrahedrite, a new variety, from the Chiprovtsi ore deposit, Western Stara-Planina mountains, Bulgaria. *Mineral. Mag.*, **40**, 233–7.
- Barton, P.B. and Skinner, B.J. (1979) Sulfide Mineral Stabilities. In *Geochemistry of Hydrothermal Ore Deposits*, (H.L. Barnes, ed.). John Wiley & Sons, New York. 278–403.
- Breskovska, V. and Tarkian, M. (1994) Compositional Variation in Bi-Bearing Fahlores. *Neues Jahrb. Mineral. Mh.*, 230–40.
- Charlat, M. and Lèvy, C. (1974) Substitutions multiples dans la série tennantite-tetraédrite. *Bull. Soc. franç. Minéral. Cristallogr.*, **97**, 241–50.
- Charnock, J.M., Garner, C.D., Patrick, R.A.D. and Vaughan, D.J. (1989) Coordination Sites of Metals in Tetrahedrite Minerals determined by EXAFS. *J. Solid State Chem.*, **82**, 279–89.
- Dana, E.S. (1896) *The System of Mineralogy*, 6th edition, 1134 pp.
- Ebel, D.S. and Sack, R.O. (1991) Arsenic-silver incompatibility in fahlore. *Mineral. Mag.*, **55**, 521–8.
- Faick, J.H. (1958) Geology of the Ord Mine, Mazatzal Mountains Quicksilver District, Arizona. *Geol. Surv. Bull.*, 1042–R.
- Frimmel, H.E. (1991) Isotopic constraints on fluid/rock ratios in carbonate rocks: Barite-sulfide mineralization in the Schwaz Dolomite, Tyrol (Eastern Alps, Austria). *Chem. Geol.*, **90**, 195–209.
- Frimmel, H.E. and Papesch, W. (1990) Sr, O, and C Isotope Study of the Brixlegg Barite Deposit, Tyrol (Austria). *Econ. Geol.*, **85**, 1162–71.
- Götzinger, M.A., Paar, W.H. and Schroll, E. (1997) 2.3. Fahlerz. In: *Handbuch der Lagerstätten der Erze, Industriemineralien und Energierohstoffe Österreichs* (L. Weber, ed.) *Archiv für Lagerstättenforschung*, **19**, 407–14.
- Grundmann, G. and Martinek, K.-P. (1994) Erzminerale und Gangarten des Bergbaubereiches Schwaz und Brixlegg. *Lapis*, **19**, 28–37.
- Gstrein, P. (1978) *Neuerkenntnisse über die Genese der Fahlerzlagerstätte Schwaz (Tirol)*. Unpub. PhD Dissertation, Univ. Innsbruck, 380 pp.
- Gstrein, P. (1979) *Neuerkenntnisse über die Genese der Fahlerzlagerstätte Schwaz (Tirol)*. *Mineral. Deposita*, **14**, 185–94.
- Gstrein, P. (1983) Über mögliche Umlagerungen von Fahlerzen im devonischen Schwazer Dolomit wie auch in der angrenzenden Schwazer Trias. *Schriftenreihe d. Erdwiss. Kommission (Austria)*, **6**, 65–73.
- Hackbarth, C. J. and Petersen, U. (1984) A fractional crystallization model for the deposition of argentinian tetrahedrite. *Econ. Geol.*, **79**, 448–60.
- Haditsch, J. G. and Mostler, H. (1969) Die Fahlerzlagerstätte auf der Gratspitz (Thierberg bei Brixlegg). *Archiv f. Lagerstättenforschung i. d. Ostalpen*, **9**, 169–94.
- Harris, D.C. (1990) Electron-microprobe analysis. In *Advanced Microscopic Studies of Ore Minerals* (J.L. Jambor and D.J. Vaughan, Eds). Mineral. Assoc. Canada Short Course Handb., **17**, 319–39.
- Heidtko, U. (1984) Die Mineralien des Landsberges bei Obermoschel (Pfalz) unter besonderer Berücksichtigung der Silberamalgame. *Aufschluss*, **35**, 191–205.
- Isser, M.v. (1905) *Schwazer Bergwerks-Geschichte. Eine Monographie über die Schwazer Erzbergbaue*. Manuscript, Museum Ferdinandeum, Innsbruck, 354 pp.
- Johnson, N.E., Craig, J.R. and Rimstidt, J.D. (1986) Compositional trends in tetrahedrite. *Canad. Mineral.*, **24**, 385–97.
- Kajiwar, Y. (1969) Fukuchilite, a new mineral from the Hanawa Mine, Akita Prefecture, Japan. *Mineral. J.*, **5**, 399–416.
- Kalbskopf, R. (1971) Die Koordination des Quecksilbers im Schwazit. *Tschermaks Mineral. Petrog. Mitt.*, **16**, 173–5.
- Kaplunnik, L.N., Pobedinskaya, E.A. and Belov, N.V. (1980) The crystal structure of Schwazite (Cu<sub>4,4</sub>Hg<sub>1,6</sub>)Cu<sub>6</sub>Sb<sub>4</sub>S<sub>12</sub>. *Dokl. Akad. Nauk SSSR*, **253**, 105–7.
- Kenngott, G.A. (1853) *Das Mohs'sche Mineralsystem, dem gegenwärtigen Standpunkte der Wissenschaft gemäss bearbeitet*, Wien.
- Krischker, G.A. (1990) *Die Baryt-Fahlerz-Lagerstätte St. Gertraudi/Brixlegg*. Unpub. Diploma Thesis, Univ. Innsbruck. 206 pp.

- Lengauer, C.L. (1988a) *Geologie und Erzmineralogie der Lagerstätte Leogang, Salzburg*. PhD Thesis, Univ. Salzburg, 146 pp.
- Lengauer, C.L. (1988b) Zur Metamorphose der westlichen Grauwackenzone (Salzburg). Abstract. *Österreich Geol. Gesell. Ann. Mtg.*, 15–16.
- Lynch, J.V.G. (1989) Large-scale hydrothermal zoning reflected in the tetrahedrite-freibergite solid solution, Keno Hill Ag-Pb-Zn district, Yukon. *Canad. Mineral.*, **27**, 383–400.
- Miller, J.W. and Craig, J.R. (1983) Tetrahedrite-tennantite series compositional variations in the Cofer Deposit, Mineral District, Virginia. *Amer. Mineral.*, **68**, 227–34.
- Moh, G.H. (1989) Ore Minerals: An experimental Approach - and new observation. *Neues Jahrbuch Mineral., Abh.*, **160**, 1–69.
- Mostler, H. (1984) An jungpaläozoischen Karst gebundene Vererzungen mit einem Beitrag zur Genese der Siderite des Steirischen Erzberges. *Geol. Paläont. Mitt. Innsbruck*, **13**, 97–111.
- Mozgova, N.N., Tsepin, A.I. and Ozerova, N.A. (1980) Arsenic Schwazite. *Dokl. Acad. Sci. USSR; Earth Sci. Sect.*, **239**, 143–6.
- Neuninger, H., Pittoni, R. and Preuschen, E. (1960) Das Kupfer der Nordtiroler Urnenfelderkultur. *Archaeologica Austriaca*, Beih. **5**, 1–89.
- Oudin, E., Marchig, V., Rösch, H., Lolou, C. and Brichet, E. (1990) Observation de  $\text{CuS}_2$  à l'état naturel dans une cheminée hydrothermale du Pacifique Sud. *C. R. Acad. Sci. Paris*, **310**, Serie II, 221–6.
- Patrick, R.A.D. and Hall, A.J. (1983) Silver substitution into synthetic zinc, cadmium and iron tetrahedrites. *Mineral. Mag.*, **47**, 441–51.
- Pirkl, H. (1961) Geologie des Triasstreifens und des Schwazer Dolomits südlich des Inn zwischen Schwaz und Wörgl (Tirol). *Jahrb. Geol. Bundesanstalt (Austria)*, **104**, 1–150.
- Pouchou, J.L. and Pichoir, F. (1984) Un nouveau modèle de calcul pour la microanalyse quantitative par spectrométrie de rayons X. *La Recherche Aéropatiale*, **3**, 167–92.
- Rammelsberg, C.F. (1849) *Repertorium des Chemischen Theils der Mineralogie*. 4th Suppl., 66–7.
- Sack, R.O. (1992) Thermochemistry of tetrahedrite-tennantite fahlores. In *The Stability of Minerals* (N.L. Ross and G.D. Price, eds), Chapman and Hall, London, 243–66.
- Schmid-Beurmann, P. and Bente, K. (1995) Stability properties of the  $\text{CuS}_2$ - $\text{FeS}_2$  solid solution series of pyrite type. *Mineral. Petrol.*, **53**, 333–41.
- Schmidegg, O. (1951) Die Erzlagerstätten des Schwazer Bergbaugesbietes, besonders des Falkenstein. *Schlern-Schriften*, **85**, 36–58.
- Schober, C. (1984) *Zur Geologie der Schwazer Trias und des Schwazer Dolomits (Tirol) unter besonderer Berücksichtigung der Vererzung*. Unpub. PhD Dissertation, Univ. Innsbruck, 186 pp.
- Schroll, E. (1979) Beitrag der Geochemie zur Kenntnis der Lagerstätten der Ostalpen. *Geol. Bundesanstalt (Austria) Verh.*, 1978, 461–70.
- Schroll, E. and Azer Ibrahim, N. (1959) Beitrag zur Kenntniss ostalpiner Fahlerze. *Tschermaks Mineral. Petrog. Mitt.*, **7**, 70–105.
- Schulz, O. (1972) Unterdevonische Baryt-Fahlerz-Mineralisation und ihre steilachsige Verformung im Grosskogel bei Brixlegg (Tirol). *Tschermaks Mineral. Petrog. Mitt.*, **18**, 114–28.
- Schulz, O. (1979) Metallogenese in den österreichischen Ostalpen. *Geol. Bundesanstalt (Austria) Verh.* 1978, 471–8.
- Seal, R.R., Essene, E.J. and Kelly, W.C. (1990) Tetrahedrite and tennantite: evaluation of thermodynamic data and phase equilibria. *Canad. Mineral.*, **28**, 725–38.
- Shimazaki, H. and Clark, L.A. (1970) Synthetic  $\text{FeS}_2$ - $\text{CuS}_2$  solid-solution and fuchuilite-like minerals. *Canad. Mineral.*, **10**, 648–64.
- Tufar, W. (1979) Mikroskopisch-lagerstättenkundliche Charakteristik ausgewählter Erzparagenesen aus dem Altkristallin, Paläozoikum und Mesozoikum der Ostalpen. *Geol. Bundesanstalt (Austria) Verh.* 1978, 499–528.
- Vasil'yev, V.I. and Lavrent'yev, Y.G. (1973) Mercury-bearing tennantite. *Dokl. Acad. Sci. USSR, Earth Sci. Sect.*, **218**, 111–3.
- Vohryzka, K. (1968) Die Erzlagerstätten von Nordtirol und ihr Verhältnis zur alpinen Tektonik. *Jahrb. Geol. Bundesanstalt (Austria)*, **111**, 3–88.
- Weidenbusch, H. (1849) Analyse des quecksilberhaltigen Fahlerzes von Schwaz in Tyrol. In *Annalen der Physik und Chemie* (J.C. Poggendorff, ed.), 3. Reihe, **16**, 86–8.
- Wu, I. and Petersen, U. (1977) Geochemistry of tetrahedrite and mineral zoning at Casapalca, Peru. *Econ. Geol.*, **72**, 993–1016.
- Zepharovich, V.v. (1859) *Mineralogisches Lexikon für das Kaiserthum Österreich. Band 1*, Wien, Verlag Milhelm Braumüller (Reprint Graz, 1985), 388–9.

[Manuscript received 6 October 1997:  
revised 10 March 1998]